Polysilicon prototypes for flip-bonded hybrid MEM-tunable filters and VCSELs

E.M. Ochoa[*], L.A. Starman, Jr.[*], W.D. Cowan[**], T.R. Nelson, Jr. [**], O. Blum Spahn[***], and J.A. Lott[*]

[*]Air Force Institute of Technology, Edward.Ochoa@afit.edu, Wright-Patterson AFB, OH
[**]Air Force Research Laboratory, Wright-Patterson AFB, OH
[***]Sandia National Laboratory, Albuquerque, NM

ABSTRACT

We characterize our novel mechanical structures for flip-bonded hybrid micro-electro-mechanically (MEM) tunable filters (MEM-TF) and MEM-tunable vertical cavity surface emitting lasers (MEM-TVCSELs) by comparing simulations with foundry fabricated actuators. Two of our prototypes, each with different flexure thickness, have analytically simulated and measured pull-in voltages of (11.6 V, 11.8 ± 0.1 V) and (8.4 V, 7.7 ± 0.5 V) respectively. We believe our hybrid approach will reduce cost, shorten development time, enable use of standard flip-chip technology and IC/MEMS foundries, and offer materials flexibility since the components do not need to be lattice matched.

Keywords: WDM, MEMS, tunable filter, tunable VCSEL, hybrid integration.

1 INTRODUCTION

Wavelength Division Multiplexing (WDM) is an effective technology to increase bandwidth by multiplexing several wavelengths through existing long-haul fiber optic networks [1, 2]. Most WDM is implemented by using multi-wavelength diode laser arrays, or widely tunable filters and diode lasers. With tunable filters and tunable diode lasers, there is no longer a need to commit to one wavelength [2]. Unfortunately, standard edge-emitting WDM laser sources require complex biasing, demand system-specific optical coupling configurations, and are difficult to manufacture [3]. This reduces system reliability, yield, and thus increases unit cost.

1.1 Monolithically-Integrated MEM-Tunable Optoelectronics

Recently, semiconductor filter and diode laser tuning has been achieved by using micro-electro-mechanical (MEM) electrostatic or magnetic actuation. Typical MEM-TF and MEM-TVCSELs operate via the electrostatic or magnetic deflection of a monolithically grown or deposited multi-layer mirror or reflector suspended by one or more flexures. As the reflector is displaced vertically, the effective optical path length is modified, thus tuning the device's fundamental resonant frequency [1, 3-7].

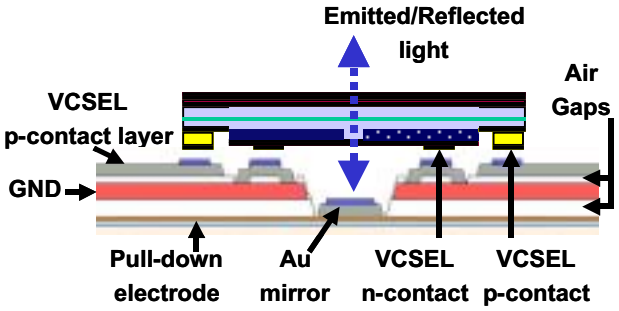

Figure 1: Design schematic of polysilicon mechanical structure for hybrid flip-bonded MEM-tunable filter or VCSEL. A VCSEL or distributed Bragg reflector (DBR) filter is bonded via co-planar contacts. Co-planar VCSEL contacts are dielectrically isolated by the air gap between the p-contact and GND layers.

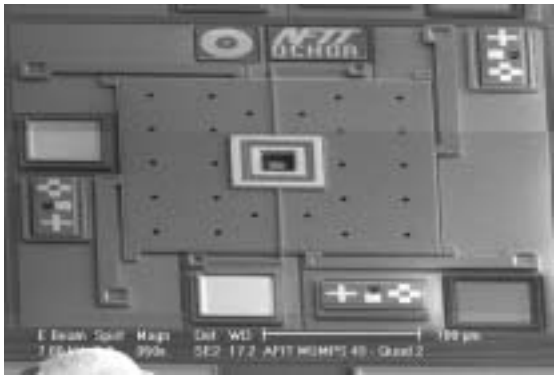

Figure 2: Scanning electron micrograph of four-flexure polysilicon actuator with centrally located, co-planar, Au ring contact pads for a flip-bonded VCSEL to be vertically actuated above an Au central reflector.

However, the disadvantages of monolithically integrated optoelectronics include high development cost, high production and equipment cost, and potentially lower performance [8]. Additionally, existing monolithic MEM-tunable semiconductor diode laser designs impose mechanical and optoelectronic fabrication trade-offs and limits on device performance.

1.2 Hybrid Integration

Within the last decade, many researchers and commercial laboratories have found the hybrid approach

more desirable. This is due to several factors. Transducer development cycles are typically much slower than CMOS, so when yield problems occur the hybrid approach allows discarding defective parts. Additionally, the development of monolithic systems is difficult and expensive [9].

Moreover, many silicon MEMS design techniques, such as the use of dimples to prevent stiction, are not yet an option for most monolithically grown MEM-TF or MEM-TVCSELs. Also, since III-V MEMS are in an entirely different material system, they are subject to different fabrication limitations, and require much technology development. Hybrid integration provides design options for MEM-TF and MEM-TVCSELs such as the flexibility to use 'best of breed' components and perform individual component optimization.

Recently, there has been significant progress in hybrid optoelectronic integration via bonding of VCSELs to integrated circuits (ICs). Flip-bonded VCSEL as large as 4x4 and 8x8 arrays have been successfully demonstrated, however, the chips require special handling after VCSEL bonding. Improvements may increase their robustness and make this technique suitable for very large arrays [8, 10].

Thus, as a first step to investigate a hybrid approach to MEM-TF and MEM-TVCSELs, we began developing designs and methods to bond III-V filters and VCSELs to polysilicon MEMS. The objective of this work is to characterize our novel prototype mechanical structures for hybrid MEM-TF and MEM-TVCSELs by validating analytic simulations with prototype mechanical structures.

2 METHODOLOGY

2.1 Design

As shown in Figures 1 and 2, our baseline design consists of a flip-bonded filter or VCSEL with co-planar contacts in an alternate instantiation of the Wilmsen, et. al [8] approach. We designed ring contacts to ensure planar-to-substrate placement and mechanical symmetry. Prototypes with MUMPs® [11] Poly 1 or Poly 2 support flexures were designed to investigate the effect of flexure thickness on actuation voltage. Also, we chose to use the MUMPs® gold layer as a fixed reflector and the filter or VCSEL as the vertically actuated element. To our knowledge, this is the first prototype design that vertically displaces the active region of a tunable diode laser rather than displacing the tuning element.

Decoupling the optical and mechanical elements prior to flip bonding enables independent optimization of resonant wavelength tuning and actuation. The fixed, lower reflector is MUMPs® Au, which is highly reflective for typical (infrared) WDM wavelengths. Since shorter wavelengths are not as highly reflected by Au, depositing alternate materials with higher reflectivity is also possible. Moreover, if the central Au reflector is raised to be co-planar to the flip-bond plane, a highly reflective DBR may be attached.

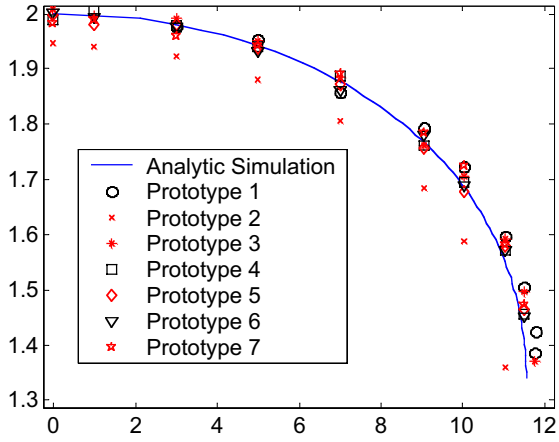

Figure 3: Comparison of analytic simulations and experimental results for seven prototypes with four Poly 1 support flexures; analytically simulated and measured pull-in voltages were 11.6 V and 11.8 ± 0.1 V respectively.

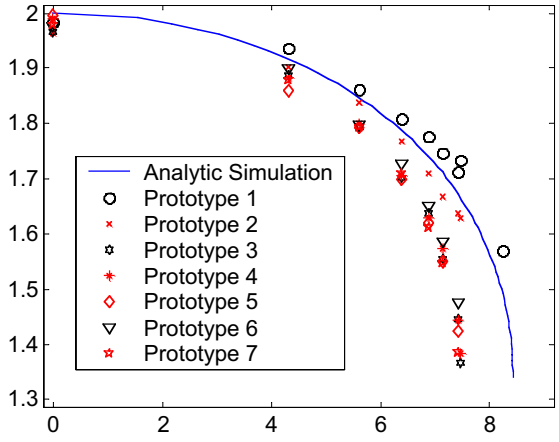

Figure 4: Comparison of analytic simulations and experimental results for seven prototypes, all with Poly 2 flexures; analytically simulated and measured pull-in voltages were 8.4 V and 7.7 ± 0.5 V respectively.

2.2 Simulation

We use the basic electrostatic piston deflection calculation to analytically model deflection dependence on actuation voltage. The basic electrostatic piston device consists of two parallel-plate electrodes separated by a dielectric gap. The movable upper electrode is supported by spring flexures with total spring constant, k. The lower electrode is fixed. The potential required for a given

deflection is given by $V=(h-d)(2kd/\_{0}A)^{1/2}$ where h is the initial air gap between electrodes, A is the overlapping electrode area, $\_{0}$ is the dielectric constant of air, $8.854\text{x}10^{-12}$ F/m, V is the voltage across the electrodes, and d is the deflection of the upper electrode toward the lower electrode. The electrostatic attractive force overwhelms the restoring force of k when $d=h/3$. The corresponding potential is the pull-in voltage, $V_{pull\text{-}in}$.

We use the transfer matrix approach of Yeh [12] to model MEM-Tunable filter or VCSEL resonant wavelength dependence on air gap thickness. This method is used to model various multilayer filter or VCSEL designs, examine the overlap of electric field intensity with gain layers, and model phase penetration depth into DBR mirrors. This method has been implemented as a suite of design tools in Matlab®.

2.3 Fabrication

As illustrated in Figure 2, fabrication is performed, but not limited to, the MUMPs® foundry [11]. On each die, we also co-locate material properties test structures (fixed-fixed beam arrays and comb-resonators) to enable characterization of each mechanical layer. We release the structures with HF, rinse with methanol, and then perform supercritical CO_2 drying. Next, we package the released die, and then characterize the material properties of test structures and our mechanical prototypes.

3 RESULTS

3.1 Actuation Characteristics

The reported MUMPs® run #43 Poly 1 and Poly 2 thickness is 1.9717 ± 0.0145 µm and 1.5088 ± 0.0075 µm respectively [13]. For the experimental die containing our prototypes and co-located material properties test structures, we characterized Young's modulus and stress of Poly 1 and Poly 2 as (125 ± 13 GPa, -4.9 ± 0.5 MPa) and (162 ± 4 GPa, -9.4 ± 0.2 MPa) respectively. We used this material data to calculate the total spring constant, k, for two sets of prototypes. The computed k for the first set of prototypes with four Poly 1 support flexures and two Poly 2 central flexures is 19.60 N/m. The computed k for the second set of prototypes with all Poly 2 flexures is 10.43 N/m. The overlapping electrode area, A, for all prototypes is 39,216 µm^2. The initial electrode air gap, h, is 2 µm. We used a ZYGO NewView 5000 interferometer to measure deflection versus actuation voltage. As shown in Figures 5 and 6, our two sets of prototypes, each with different flexure thickness, have analytically simulated and measured pull-in voltages of (11.6 V, 11.8 ± 0.1 V) and (8.4 V, 7.7 ± 0.5 V) respectively. As shown in Figures 5 and 6, using all Poly 2 flexures reduces pull-in voltage by approximately 4 V.

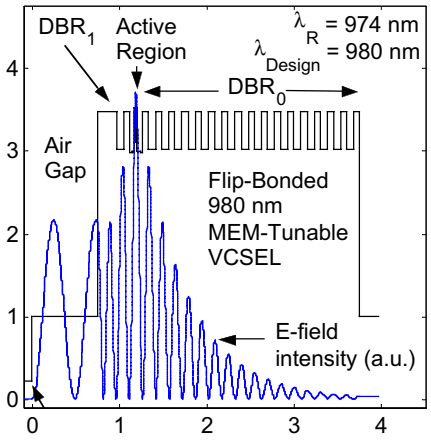

Figure 5: Simulated E-field intensity at 974 nm resonant wavelength, $\_{R}$, for 0.75 µm thick air gap in a flip-bonded 980 nm hybrid MEM-tunable VCSEL. DBR_0 is 16.5 pairs of $Al_{0.1}Ga_{0.9}As/Al_{0.9}Ga_{0.1}As$, and DBR_1 is 1.5 pairs of $Al_{0.1}Ga_{0.9}As/Al_{0.9}Ga_{0.1}As$.

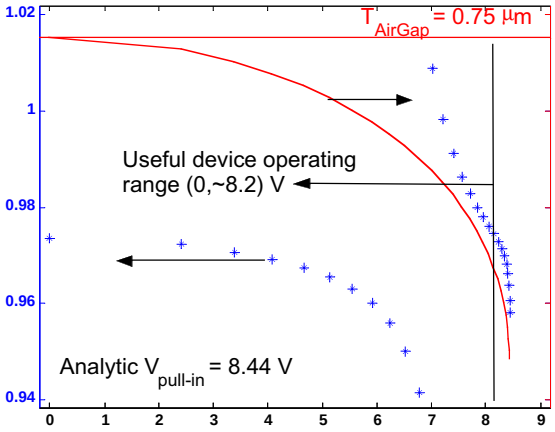

Figure 6: Simulated resonant wavelength tuning for 0.75 µm (initial) air gap, flip-bonded 980 nm hybrid MEM-tunable VCSEL with 1.5 µm thick flexures.

Finally, to investigate the effect of initial air gap between the flip-bonded MEM-TVCSEL and central reflector, we successfully fabricated five prototype Au reflectors. Each prototype provides one of the following tunable air gap's initial thickness, T_{AirGap}: 0.75, 1.25, 2.0, 3.25, or 5.25 µm.

3.2 Simulated Tuning Characteristics

Since the second set of prototypes with all Poly 2 flexures have lower actuation voltage characteristics, we simulated a 980 nm flip-bonded MEM-TVCSEL to investigate the

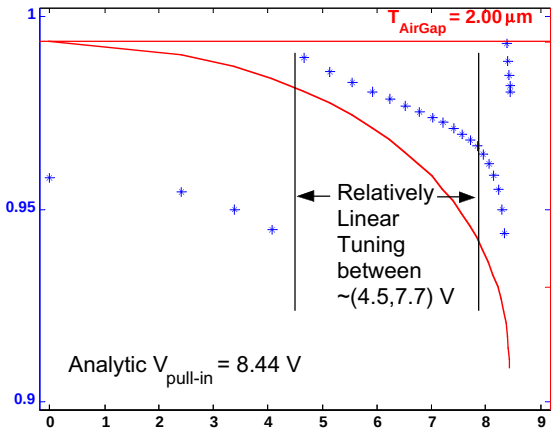

Figure 7: Simulated resonant wavelength tuning for 2.00 µm (initial) air gap, flip-bonded 980 nm MEM-tunable VCSEL with 1.5 µm thick flexures. Relatively linear resonant wavelength tuning is due to the interaction between the parabolic deflection of the actuator and the device's periodic, nonlinear resonant wavelengths.

corresponding T_{AirGap} design trade-offs. Note, however, hybrid MEM-TFs or MEM-TVCSELs are not limited to tuning near 980 nm since one may use a custom central reflector as discussed in Section 2.1. As shown in Figure 5, for each air gap thickness, we calculate the corresponding resonant wavelength and electric field intensity through the device. As shown in Figures 6 and 7, our simulations indicate the choice of T_{AirGap} significantly influences tuning characteristics, potentially leading to a relatively linear tuning response to actuation voltage. This is most apparent in Figure 7 which shows resonant wavelength tuning from 989 nm to 964 nm corresponding to control voltages of 4.5 V to 7.7 V with less than 1.3 nm deviation from linearity. This linear tuning characteristic is desirable from a control perspective, and was identified due to our decoupled optical and mechanical hybrid MEM-TF and MEM-TVCSEL design methodology. Finally, we also simulated 980 nm monolithically-fabricated MEM-TVCSELs and confirmed the choice of T_{AirGap} leads to similar linear tuning operating regions.

4 CONCLUSIONS

Our novel polysilicon mechanical prototypes are good candidates for flip-bonded hybrid MEM-tunable filters and VCSELs. Resonance wavelength tuning is accomplished by vertically reducing air gap thickness. Key advantages include enabling the use of MUMPs® dimples to reduce stiction, independent design and optimization of mechanical and optical elements, and identical mechanical prototypes may be used in different multi-wavelength applications. This work is sponsored by the Air Force Research Laboratory, the Air Force Office of Scientific Research, and Sandia National Laboratory. The views expressed in this article are those of the author and do not reflect the official policy or position of the United States Air Force, Department of Defense, or the US Government. Sandia is a multiprogram laboratory operated by Sandia Corporation, a Lockheed Martin Company, for the United States Department of Energy under contract DE-AC04-94AL85000

REFERENCES

[1] C.J. Chang-Hasnain, "Tunable VCSEL," *IEEE Journal On Selected Topics in Quantum Electronics*, vol. 6, no. 6, pp. 978–987, November/ December 2000.

[2] A. Martin, "By itself, DWDM does not spell success," *Laser Focus World*, May 2001.

[3] C.J. Chang-Hasnain, *Micromechanical Tunable VCSEL*, chapter 6, pp. 279–318, Optoelectronic Properties of Semiconductors and Superlattices. Gordon and Breach Science Publishers, 2000.

[4] P. Tayebati, "Half-symmetric cavity tunable microelectromechanical VCSEL with single spatial mode," *IEEE Photonics Technology Letters*, vol. 10, no. 12, pp. 1679–1681, December 1998.

[5] S. Jin and H. Mavoori, "Magnetically tunable and latchable broad range semiconductor laser," U.S. Patent and Trademark Office, November 2000, Patent Number: 6,154,471.

[6] J. Berger, Y. Zhang, J. Grade, H. Lee, S. Hrinya, H. Jerman, A. Fennema, and A. Tselikov, "Micro external cavity laser (ECL) presentation," iolon Products: Literature and Presentations, March 2001, www.iolon.com/ppt/ofc jberger.pps.

[7] J.A. Lott, M.J. Noble, E.M. Ochoa, L.A. Starman, and W.D. Cowan, "Tunable red vertical cavity surface emitting lasers using flexible micro-electro-mechanical top mirrors," in *IEEE Optical MEMS*, Kauai, Hawaii, August 2000.

[8] C.W. Wilmsen, *Vertical-Cavity Surface Emitting Lasers*, chapter 12, pp. 417–448, Cambridge University Press, 1999.

[9] W. Lang, "Reflections on the future of microsystems," *Sensors and Actuators: A* (Physical), vol. 72, pp. 1–15, 1999.

[10] R. Pu, E.M. Hayes, R. Jurrat, C.W. Wilmsen, K.D. Choquette, H.Q. Hou, and K.M. Geib, "VCSELs bonded directly to foundry fabricated GaAs smart pixel arrays," *IEEE Photonics Technology Letters*, vol. 9, no. 12, pp. 1622–1624, December 1997.

[11] D.A. Koester, R. Mahadevan, B. Hardy, and K.W. Markus, *MUMPs Design Handbook, Revision 7.0*, Cronos Integrated Microsystems, 2001, www.memsrus.com.

[12] P. Yeh, Optical Waves in Layered Media, Wiley: New York, 1988.

[13] MUMPs® 43 Run data, Cronos Integrated Microsystems, 2001, www.memsrus.com.